Absolute measurement of the transient optical nonlinearity in N₂, O₂, N₂O, and Ar

J. K. Wahlstrand, Y.-H. Cheng, and H. M. Milchberg

Institute for Research in Electronics and Applied Physics, University of Maryland, College Park, Maryland 20742, USA

The absolute time-dependent nonlinear response of O_2, N_2, N_2O, and Ar to intense nonionizing, ultrashort optical pump pulses is measured with single-shot spectral interferometry. The instantaneous and delayed rotational responses are distinguished as a function of pump-pulse duration and probe central wavelength. Our measurements are central to the modeling and understanding of nonlinear propagation of intense ultrashort laser pulses in gases.

PACS number(s): 42.65.An, 42.65.Jx, 42.65.Re

I. INTRODUCTION AND BACKGROUND

The nonlinear optical response of gases plays a role in a variety of phenomena under wide investigation for applications, including harmonic generation and attosecond physics [1], femtosecond filamentation [2], and pulse compression [3]. Recently, we demonstrated [4] that the instantaneous nonlinear polarizability of Ar and N_2 is dominantly second order in the laser field amplitude for optical laser intensity all the way up to the ionization threshold. The total response is composed of instantaneous and delayed parts, which are, respectively, the nonlinear distortion of the atomic or molecular electron cloud (electronic response) and field-induced molecular rotation, with a weak, fast contribution from adiabatic (prompt) bond stretching. Together, these responses are called the optical Kerr nonlinearity. Despite the extensive activity employing nonlinear laser-gas interactions, the Kerr nonlinearity, especially in molecular gases, is still not known with much precision. Commonly used values for the instantaneous and delayed contributions to the Kerr nonlinearity vary significantly. Improving the precision of these numbers is critical for calculations of the propagation of intense laser pulses in gases, which depend extremely sensitively on them [5–9].

In this paper, we present absolute measurements of the optical nonlinearity in O_2, N_2, N_2O, and Ar. Our method can be extended to most transparent media provided the sample is thin enough. Here, we determine accurate values of the instantaneous Kerr coefficient n_2 and the molecular polarizability asymmetry $\Delta\alpha = \alpha_\parallel - \alpha_\perp$, where $\alpha_\parallel$ and $\alpha_\perp$ are the linear polarizabilities along and across the molecular bond axis.

In all of the gases studied here, the first ionization potential is far above the laser photon energy of 1.55 eV. As a result, the nonlinear response of the electronic states is essentially instantaneous and is characterized in terms of the Kerr coefficient n_2. In addition, molecular gases can have an important, even dominant, response due to the alignment and stretching of the molecular bonds in the intense laser field [10–12]. This response can be described by a time-domain Raman response function $R(t)$. The total nonlinear index of refraction, to second order in the field or first order in the laser intensity, is

$$\Delta n(t) = n_2 I(t) + \int_{-\infty}^{\infty} R(t - t') I(t') dt', \qquad (1)$$

where $I(t)$ is the laser intensity. The orientational (bond stretch and molecular alignment) contribution to the instantaneous

electronic response is fourth order in the field amplitude and is negligible on the time scale of the $n_2 I(t)$ response [13]. In the gases studied here, the small adiabatic bond stretch contribution to $R(t)$ cannot be separated out because the spacing between vibrational states is much greater than the bandwidth corresponding to our 40-fs FWHM pump pulse. At high intensity, there is an additional contribution from free electrons generated by ionization [4], but for all data presented later, the intensity is kept below the ionization threshold.

II. EXPERIMENTAL TECHNIQUE

Many techniques have been used to measure the nonlinear refractive index of gases, including measurements of self-focusing [14], spectral changes caused by self–phase modulation [10,15], and pump-probe experiments measuring spectral or polarization changes in a weak probe pulse due to cross-phase modulation [11,16]. We use single-shot supercontinuum spectral interferometry (SSSI) [13,17,18], which enables the measurement, with micron spatial resolution and femtosecond time resolution, of the time-dependent phase imparted to a probe pulse by the transient response of a medium excited by a copropagating pump pulse. In our experiment, the interaction takes place in a very thin gas flow of effective thickness $L_{\rm eff} \ll d_{\rm c,\,pump}$, where $d_{\rm c,\,pump}$ is the confocal parameter. Therefore, the pump intensity is axially uniform along the interaction length [4], and the measured probe phase shift is

$$\Delta\Phi(x,t) = k_0 \int \Delta n(x,z,t) dz = k_0 \Delta n_{\rm atm}(x,t) \int \frac{P(z)}{P_0} dz$$
$$= k_0 \Delta n_{\rm atm}(x,t) L_{\rm eff}, \qquad (2)$$

where x is the transverse coordinate in the sample, z is the axial coordinate along the interaction, k_0 is the average vacuum wavenumber of the chirped probe pulse over the frequency range it overlaps with the pump pulse, $P(z)$ is the pressure distribution, and $\Delta n_{\rm atm}(x,t)$ is the change in refractive index at atmospheric pressure P_0. We note that experiments with $L_{\rm eff} \gg d_{\rm c}$, which is the case for most gas cells [11,13,16,18], suffer from two main problems: (i) the three-dimensional pump and probe beam profiles are imprecisely known, and (ii) even if known, nonlinear pump propagation would distort them. In any case, $\Delta\Phi$ will be a complicated mixed space-time average.

The laser is a 1-kHz repetition rate Ti:sapphire amplifier producing 40-fs, 3.5-mJ pulses. A supercontinuum (SC) with a usable bandwidth of 120 nm is generated by filamentation

in SF_6 [19]. Probe and reference SC pulses, separated by ~ 2 ps, are generated using a Michelson interferometer. The pump, probe, and reference pulses are collinearly combined using a dichroic mirror and focused (such that $d_{c,probe} > d_{c,pump}$ and probe spot > pump spot) into the thin gas flow in a vacuum chamber pumped by a roots blower. A $\lambda/2$ wave plate in the pump path allows rotation of the pump polarization. The gas flow target consists of a stainless steel tube with 90-μm-thick walls. A section of the tube is flattened, and 80-μm-diameter entrance and exit holes are laser drilled through it. With an input flow pressure of 1 atm in the tube, the background pressure in the chamber is ~ 200 mTorr. The reference pulse precedes the pump, which is temporally overlapped with the probe. After the tube, the pump is spectrally filtered from the beam, and the interaction zone is imaged onto the entrance slit of an imaging spectrometer and relayed to a CCD at the spectrometer's focal plane, where the probe and reference interfere in the frequency domain. The time-domain phase shift $\Delta\Phi(x,t)$ is then found from the change in the spectral phase and amplitude extracted from this interferogram and from the probe spectral phase [17]. The latter is found from the dependence of the change in probe spectral phase on pump-probe time delay. The probe spectral phase is quadratic, with a group-delay dispersion of 1750 fs^2. We average 1000 interferograms before performing the extraction [18], allowing measurement of phase shifts smaller than possible in a single shot. The dominant source of noise in a single-shot measurement is CCD pixel noise.

To measure the spatial distribution of the pump intensity without relying on external imaging of the focal spot, we measure the instantaneous Kerr phase shift along two perpendicular slices, $\Delta\Phi(x,t)$ and $\Delta\Phi(y,t)$, using a Dove prism to rotate the image on the spectrometer slit. We find that the pump spot size at the target is 29 μm × 27 μm. This is shown in Figs. 1(a) and 1(b). The beam profile measured is used to find the relation between the pulse fluence and the peak intensity.

A folded wave-front interferometer employing a 635-nm cw diode laser was used to measure L_{eff} in the flow tube. The portion of the beam passing through the hole interfered with light passing outside the tube, and the hole was imaged to a CCD camera as shown in Fig. 1. Interferograms were captured at a frame rate of 14.5 s^{-1} as the gas flow into the tube is suddenly shut off. The difference in phase between the initial state of steady flow and long times after shut off, when the tube is evacuated, can be expressed as $\Delta\varphi = k_0 n_0 L_{eff}$, where n_0 is the refractive index at 1 atm. Measuring $\Delta\varphi = 1.16$ rad and using $n_0 - 1 = 2.795 \times 10^{-4}$ for 633 nm in N_2 at 1 atm [20], we find $L_{eff} = 418$ μm. Using this value for L_{eff} with our spectral interferometry phase shifts gives absolute values of Kerr nonlinearity at 1 atm. (Since the outer thickness of the tube is 475 μm, this implies an average pressure inside the tube of slightly less than 1 atm.)

With an absolute measurement of nonlinearity in N_2 from the thin gas flow, we can perform relative phase-shift measurements in all other gases with the vacuum chamber backfilled at low pressure (here ~ 90 Torr) and reference the phase shifts to the flow-tube measurement, allowing a higher signal-to-noise ratio. There was no measurable phase front distortion of the pump due to self-focusing (peak power is $\sim 1\%$ of critical at 90 Torr). Lineouts of the phase shift measured for
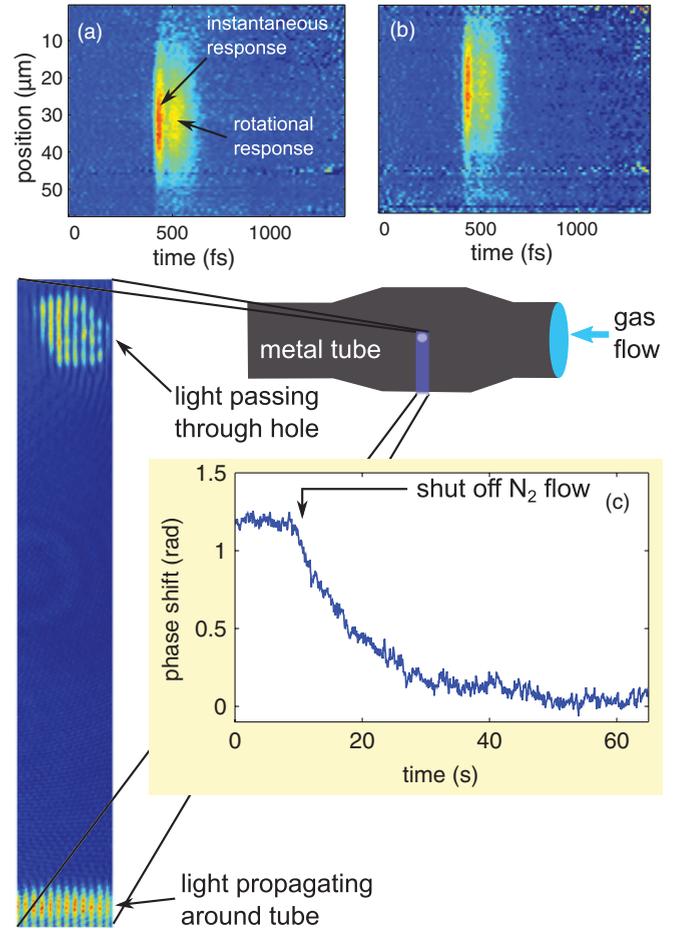

FIG. 1. (Color online) Measurement of absolute phase shifts in N_2 using a 475-μm-thick gas target with $L_{eff} = 418$ μm. (a, b) Nonlinear phase shift extracted using SSSI at peak laser intensity 41 TW/cm^2 along two perpendicular slices x and y through the probe spot. (c) Linear phase shift due to the gas in the tube, measured using folded wave-front interferometry, with a CCD camera taking data at 14.5 frames s^{-1}. The inset shows a schematic of the flow tube and an example interferogram.

each gas for pump parallel (black solid line) and perpendicular (blue dashed line) to probe are shown in Fig. 2. Scaling the N_2 backfill data to match the flow tube data, we find an effective interaction length at 90 Torr of 4.41 mm, which is used for the rest of the gases. Using the gas flow target here and in our prior work [4], we have found within error that the nonlinear response, both instantaneous and rotational, is linear in the intensity up to the ionization threshold for all gases studied. Thus, to extract absolute Kerr coefficients from our data, we keep the laser intensity well below the ionization threshold.

III. RESULTS AND DISCUSSION

As shown in Eq. (1), the response is composed of instantaneous and rotational parts. To separate these contributions, we recognize that if $\Delta\Phi_\parallel = \Delta\Phi_{inst} + \Delta\Phi_{rot}$ for probe polarization parallel to the pump, then symmetry properties of the nonlinear susceptibility tensor [21] imply $\Delta\Phi_\perp = \Delta\Phi_{inst}/3 - \Delta\Phi_{rot}/2$ for probe polarized perpendicular to
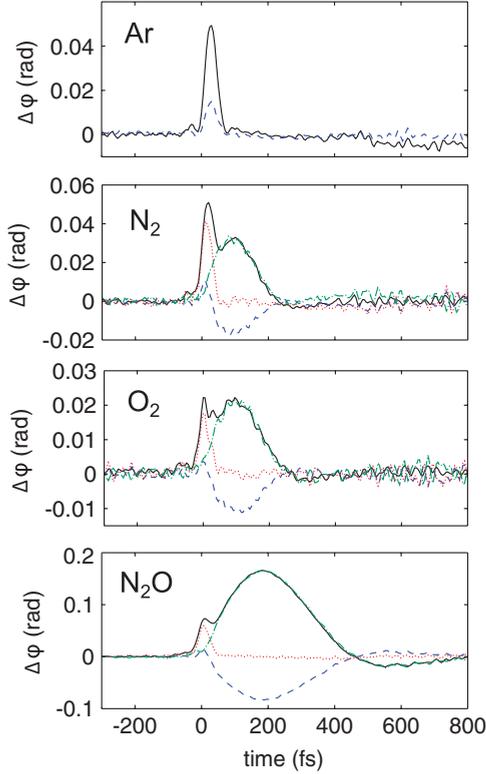
FIG. 2. (Color online) Lineouts showing the phase shift $\Delta\Phi(t)$ for pump polarization parallel to probe (solid black line) and pump perpendicular to probe (blue dashed line). Also shown is the decomposition of the signal into the instantaneous (red dotted line) and rotational (green dash-dotted line) signals, as described in the text. The pressure used for each gas was 90 Torr. The peak intensity used for each gas was Ar, 41 TW/cm^2; N$_2$, 45 TW/cm^2; O$_2$, 14 TW/cm^2; and N$_2$O, 28 TW/cm^2.

pump. These equations yield $\Delta\Phi_{\rm inst} = 3(\Delta\Phi_{\parallel} + 2\Delta\Phi_{\perp})/5$ and $\Delta\Phi_{\rm rot} = 2(\Delta\Phi_{\parallel} - 3\Delta\Phi_{\perp})/5$. These are shown in Fig. 2 as red dotted ($\Delta\Phi_{\rm inst}$) and green dash-dotted ($\Delta\Phi_{\rm rot}$) lines. The instantaneous response is proportional to the temporal shape of the pulse $I(t)$, and the small bump at early time delays has been verified as a real feature of the laser pulse using spectral phase interferometry for direct electric-field reconstruction [22].

We fit the delayed response to the second term in Eq. (1). The rotational part of $R(t)$ is proportional to the ensemble average molecular alignment $\langle\cos^2\theta\rangle - 1/3$ calculated using a density matrix code [23], where θ is the angle between the molecular axis and the optical field direction. The only inputs to the code are $\Delta\alpha$ and the molecular moment of

inertia, where the latter is known to high accuracy from rotational spectroscopy [24]. We find the values of $\Delta\alpha$ from the simulations that best match experiment. [There is no delayed vibrational response contributing to $R(t)$ because the bandwidth of the pump pulse is not sufficient to excite vibrational modes.]

We attribute the instantaneous phase shift to the electronic response because the adiabatic bond stretch contribution is small: using the rovibrational response function plotted in [12] to simulate the instantaneous phase shift due to adiabatic bond stretching in N$_2$ and O$_2$ gives a result $\sim$30 times smaller than our measured instantaneous phase shift. This is consistent with Shelton and Rice [25], who showed that neglecting the vibrational component of the Kerr effect results in errors in the nonlinear susceptibility of less than 10%.

Our results are summarized in Table I. The largest source of uncertainty is the peak intensity, which depends on the laser spot size, average power, and pulse width. The error is reduced by employing the full transverse profile of the intensity as measured in Figs. 1(a) and 1(b), for example. Note that the uncertainty values given in Table I are the absolute error; the relative contribution between n_2 and $\Delta\alpha$ was measured much more precisely because it does not depend on the peak intensity. Ratios of values between gases are also more precise than the absolute error given because the focusing conditions were identical. In the limit of a long pulse, the rotational response is adiabatic, and the effective instantaneous Kerr coefficient has both electronic and rotational components. One can show using a perturbative calculation [13] that

$$n_{2,\rm long} = n_2 - \frac{8\pi N(\Delta\alpha)^2}{15 n_0^2 c^2 \hbar B}$$
$$\times \left[\sum_j \frac{j(j-1)}{(2j-1)^2}\left(\frac{\rho_j^{(0)}}{2j+1} - \frac{\rho_{j-2}^{(0)}}{2j-3}\right)\right],$$

where N is the gas density, B is the rotational constant, and

$$\rho_j^{(0)} = \frac{D_j(2j+1)e^{-hcBj(j+1)/k_BT}}{\sum_k D_k(2k+1)e^{-hcBk(k+1)/k_BT}},$$

where k_B is Boltzmann's constant, T is the gas temperature, and D_j is a statistical weighting factor that depends on nuclear spin. The ratio of n_2 to $n_{2,\rm long}$ for each gas at atmospheric density and room temperature, calculated from our measured values of n_2 and $\Delta\alpha$, is also shown in Table I. We use $B = 2.0$ cm^{-1} for N$_2$, $B = 1.44$ cm^{-1} for O$_2$, and $B = 0.41$ cm^{-1} for N$_2$O [26].

TABLE I. The measured Kerr coefficient n_2, polarizability anisotropy $\Delta\alpha$, and the ratio of the effective n_2 values for a short pulse to a long pulse for each gas studied and a comparison with previous experimental and theoretical work.

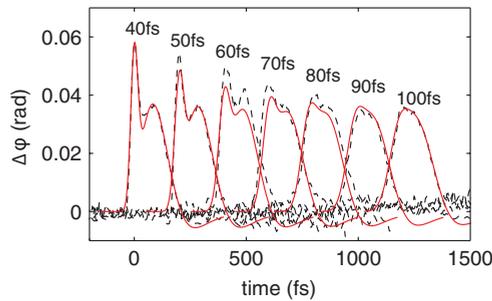| Gas	n_2 (10^{-20} cm^2/W)				$\Delta\alpha$ (10^{-25} cm^3)		$n_2/n_{2,\rm long}$
	This work	Nibbering *et al.* [10]	Loriot *et al.* [16]	Shelton and Rice [25]	This work	Lin *et al.* [26]	This work
Ar	9.7 ± 1.2	14 ± 2	10.0 ± 0.9	10.4			
N$_2$	7.4 ± 0.9	23 ± 3	11 ± 2	8.1	6.7 ± 0.3	9.3	0.23
O$_2$	9.5 ± 1.2	51 ± 7	16.0 ± 3.5	8.7	10.2 ± 0.4	11.4	0.14
N$_2$O	17.2 ± 2.2				28.1 ± 1.1	27.9	0.04

FIG. 3. (Color online) Pulse-width dependence of the nonlinear response in N_2. Measured phase shift extracted using SSSI (black dashed line), with the pulse width varied between 40 and 100 fs by adjusting the compressor. The pulse energy is kept constant. Also shown is the phase shift calculated (red solid line) using Eq. (1) and the parameters (n_2, $\Delta\alpha$) measured with a 40-fs pulse.

Previous measurements of n_2 in the gases studied here varied widely [10,11,16], in part because ~100-fs pulses were used, and thus the instantaneous response was difficult to separate reliably from the rotational response. In addition, several techniques [10,15] depend sensitively on three-dimensional nonlinear propagation effects. In general, a possible source of error in pump-probe measurements arises from using degenerate pump and probe pulses. This can lead to spurious results from two-beam coupling through an intensity or plasma grating [27].

Possible dispersion in the nonlinear susceptibility was addressed by simply changing the pump-probe time delay. This varied the SC probe wavelength band temporally overlapping the pump. There was no measurable variation, to within error, in n_2 or $\Delta\alpha$ over the central probe wavelength range of 550–635 nm for any of the gases studied. This is consistent with dispersion estimates using a power series expression [25,28], showing that for a SC probe at a central wavelength of 580 nm, we overestimate n_2 at 800 nm by less than 3%, smaller than our error bars.

It is interesting to consider how the electronic response merges with the rotational as the pump pulse duration increases. Previously, the pulse-width dependence of the Kerr effect had been probed only indirectly by measurements of critical power in self-focusing [12,29]. However, it was recently shown that critical power measurements can be complicated by defocusing effects from plasma generation [30]. Figure 3 shows the pump–pulse-width–dependent response of N_2, with the pump energy kept constant. It is seen that for pulses longer than ~80 fs, the instantaneous response merges with the rotational. This is consistent with prior work with ~100-fs pulses [13,18,24] and applies to the vast majority of filamentation experiments in air [2]. The results of Fig. 3 also allow us to test the validity of Eq. (1), whose curves are overlaid on the experimental curves. The experimental results are in good agreement with the simulations.

IV. CONCLUSIONS

In summary, we have presented direct measurements of the optical nonlinearity in the major components of air and N_2O using supercontinuum spectral interferometry. Our measurements indicate that the instantaneous response in these gases was overestimated in previous experiments that directly measured the Kerr coefficient, probably because of the use of longer pulses. Our measurements agree to within error with previous experiments that use harmonic generation and a theoretical model for the dispersion of the third-order susceptibility [24]. Our results should significantly improve simulations of pulse compression and filamentation in these gases, with special application to atmospheric propagation.

ACKNOWLEDGMENTS

[1] T. Brabec and F. Krausz, Rev. Mod. Phys. **72**, 545 (2000).

[2] A. Couairon and A. Mysyrowicz, Phys. Rep. **441**, 47 (2007).

[3] M. Nisoli, S. De Silvestri, O. Svelto, R. Szipocs, K. Ferenczy, C. Spielmann, S. Sartania, and F. Krausz, Opt. Lett. **22**, 522 (1997).

[4] J. K. Wahlstrand, Y. H. Cheng, Y. H. Chen, and H. M. Milchberg, Phys. Rev. Lett. **107**, 103901 (2011).

[5] M. Mlejnek, E. M. Wright, and J. V. Moloney, Opt. Lett. **23**, 382 (1998).

[6] J. R. Penano, P. Sprangle, P. Serafim, B. Hafizi, and A. Ting, Phys. Rev. E **68**, 056502 (2003).

[7] J. R. Penano, P. Sprangle, B. Hafizi, A. Ting, D. F. Gordon, and C. A. Kapetanakos, Phys. Plasmas **11**, 2865 (2004).

[8] A. Couairon and L. Berge, Phys. Plasmas **7**, 193 (2000).

[9] Y.-H. Chen, S. Varma, T. M. Antonsen, and H. M. Milchberg, Phys. Rev. Lett. **105**, 215005 (2010).

[10] E. T. J. Nibbering, G. Grillon, M. A. Franco, B. S. Prade, and A. Mysyrowicz, J. Opt. Soc. Am. B **14**, 650 (1997).

[11] J. Ripoche, G. Grillon, B. Prade, M. Franco, E. Nibbering, R. Lange, and A. Mysyrowicz, Opt. Commun. **135**, 310 (1997).

[12] A. M. Zheltikov, Opt. Lett. **32**, 2052 (2007).

[13] Y. Chen, S. Varma, A. York, and H. M. Milchberg, Opt. Express **15**, 11341 (2007).

[14] W. Liu and S. Chin, Opt. Express **13**, 5750 (2005).

[15] M. Shaw, C. Hooker, and D. Wilson, Opt. Commun. **103**, 153 (1993).

[16] V. Loriot, E. Hertz, O. Faucher, and B. Lavorel, Opt. Express **17**, 13429 (2009); **18**, 3011 (2010).

[17] K. Y. Kim, I. Alexeev, and H. M. Milchberg, Appl. Phys. Lett. **81**, 4124 (2002).

[18] Y. Chen, S. Varma, I. Alexeev, and H. Milchberg, Opt. Express **15**, 7458 (2007).

[19] N. Zhavoronkov, Opt. Lett. **36**, 529 (2011).

[20] Y. Clergent, C. Durou, and M. Laurens, J. Chem. Eng. Data **44**, 197 (1999).

[21] R. L. Sutherland, *Handbook of Nonlinear Optics* (Marcel Dekker, New York, 1996).

[22] C. Iaconis and I. Walmsley, IEEE J. Quantum Electron. **35**, 501 (1999).

[23] The nonperturbative density matrix calculation, for a 40-fs FWHM pulse and temperature of 300 K, includes rotational states up to $j_{max} = 30$ for N_2 and O_2 and $j_{max} = 45$ for N_2O.

[24] S. Varma, Y. H. Chen, and H. M. Milchberg, Phys. Rev. Lett. **101**, 205001 (2008).

[25] D. P. Shelton and J. E. Rice, Chem. Rev. **94**, 3 (1994).

[26] C. H. Lin, J. P. Heritage, T. K. Gustafson, R. Y. Chiao, and J. P. McTague, Phys. Rev. A **13**, 813 (1976).

[27] J. K. Wahlstrand and H. M. Milchberg, Opt. Lett. **36**, 3822 (2011).

[28] D. M. Bishop, J. Chem. Phys. **90**, 3192 (1989).

[29] D. E. Laban, W. C. Wallace, R. D. Glover, R. T. Sang, and D. Kielpinski, Opt. Lett. **35**, 1653 (2010).

[30] P. Whalen, J. V. Moloney, and M. Kolesik, Opt. Lett. **36**, 2542 (2011).